Molecular interactions governing the incorporation of cholecalciferol and retinyl-palmitate in mixed taurocholate-lipid micelles

Charles Desmarchelier, Véronique Rosilio, David Chapron, Ali Makky, Damien Preveraud, Estelle Devillard, Véronique Legrand-Defretin, Patrick Borel

Molecular interactions governing the incorporation of cholecalciferol and retinyl-palmitate in mixed taurocholate-lipid micelles

Charles Desmarchelier[1], Véronique Rosilio[2*], David Chapron[2], Ali Makky[2], Damien P. Prévéraud[3], Estelle Devillard[3], Véronique Legrand-Defretin[3], Patrick Borel[1]

[1] NORT, Aix-Marseille University, INRA, INSERM, 13005, Marseille, France.

[2] Institut Galien Paris Sud, UMR 8612, Univ Paris-Sud, CNRS, Université Paris-Saclay, 5 rue J.-B. Clément, 92290 Châtenay-Malabry, France.

[3] Adisseo France S.A.S., Center of Expertise and Research in Nutrition, 6 route Noire, 03600 Commentry, France.

***Corresponding author**: Véronique Rosilio, Université Paris-Sud, UMR CNRS 8612, Université Paris-Saclay, 5 rue J-B. Clément, 92296 Châtenay-Malabry Cedex FRANCE.

Tel : +33 1 46 83 54 18. E-Mail: veronique.rosilio@u-psud.fr

Abbreviations: NaTC (sodium taurocholate), RP (retinyl palmitate), D_3 (cholecalciferol), cmc (critical micelle concentration), cac (critical aggregation concentration), LDP (lipid digestion products), PC (phosphatidylcholine), Lyso-PC (L-α-lysophosphatidylcholine palmitoyl), POPC (2-oleoyl-1-palmitoyl-sn-glycero-3-phosphocholine).

Abstract

Cholecalciferol (D_3) and retinyl palmitate (RP) are the two main fat-soluble vitamins found in foods from animal origin. It is assumed that they are solubilized in mixed micelles prior to their uptake by intestinal cells, but only scarce data are available on the relative efficiency of this process and the molecular interactions that govern it. The extent of solubilization of D_3 and RP in micelles composed of lipids and sodium taurocholate (NaTC) was determined. Then, the molecular interactions between components were analyzed by surface tension and surface pressure measurements. The mixture of lipids and NaTC allowed formation of micelles with higher molecular order, and at lower concentrations than pure NaTC molecules. D_3 solubilization in the aqueous phase rich in mixed micelles was several times higher than that of RP. This was explained by interactions between NaTC or lipids and D_3 thermodynamically more favorable than with RP, and by D_3 self-association.

Keywords: bioaccessibility; surface pressure; bile salt; compression isotherm; lipid monolayer; vitamin A; vitamin D; phospholipid.

1. Introduction

Retinyl esters and cholecalciferol (D_3) (Figure 1) are the two main fat-soluble vitamins found in foods of animal origin. There is a renewed interest in deciphering their absorption mechanisms because vitamin A and D deficiency is a public health concern in numerous countries, and it is thus of relevance to identify factors limiting their absorption to tackle this global issue. The fate of these vitamins in the human upper gastrointestinal tract during

digestion is assumed to follow that of dietary lipids (Borel *et al.* 2015). This includes emulsification, solubilization in mixed micelles, diffusion across the unstirred water layer and uptake by the enterocyte via passive diffusion or apical membrane proteins (Reboul *et al.* 2011). Briefly, following consumption of vitamin-rich food sources, the food matrix starts to undergo degradation in the acidic environment of the stomach, which contains several enzymes, leading to a partial release of these lipophilic molecules and to their transfer to the lipid phase of the meal. Upon reaching the duodenum, the food matrix is further degraded by pancreatic secretions, promoting additional release from the food matrix, and both vitamins then transfer from oil-in-water emulsions to mixed micelles (and possibly other structures, such as vesicles, although not demonstrated yet). As it is assumed that only free retinol can be taken up by enterocytes, retinyl esters are hydrolyzed by pancreatic enzymes, namely pancreatic lipase, pancreatic lipase-related protein 2 and cholesterol ester hydrolase (Desmarchelier *et al.* 2013). Bioaccessible vitamins are then taken up by enterocytes via simple passive diffusion or facilitated diffusion mediated by apical membrane proteins (Desmarchelier *et al.* 2017). The apical membrane protein(s) involved in retinol uptake by enterocytes is(are) yet to be identified but in the case of D_3, three proteins have been shown to facilitate its uptake: NPC1L1 (NPC1 like intracellular cholesterol transporter 1), SR-BI (scavenger receptor class B member 1) and CD36 (Cluster of differentiation 36) (Reboul & Borel 2011). Both vitamins then transfer across the enterocyte towards the basolateral side. The transfer of vitamin A is mediated, at least partly, by the cellular retinol-binding protein, type II (CRBPII), while that of vitamin D is carried out by unknown mechanisms. Additionally, a fraction of retinol is re-esterified by several enzymes (Borel & Desmarchelier 2017). Vitamin A and D are then incorporated in chylomicrons in the Golgi apparatus before secretion in the lymph.

The solubilization of vitamins A and D in mixed micelles, also called micellarization or micellization, is considered as a key step for their bioavailability because it is assumed that the

non-negligible fraction of fat-soluble vitamin that is not micellarized is not absorbed (Desmarchelier *et al.* 2013). Mixed micelles are mainly made of a mixture of bile salts, phospholipids and lysophospholipids, cholesterol, fatty acids and monoglycerides (Hernell *et al.* 1990). These compounds may form various self-assembled structures, e.g., spherical, cylindrical or disk-shaped micelles (Walter *et al.* 1991, Leng *et al*. 2003) or vesicles, depending on their concentration, the bile salt/phospholipid ratio (Walter *et al.* 1991), the phospholipid concentration, but also the ionic strength, pH and temperature of the aqueous medium (Madency & Egelhaaf 2010; Salentinig *et al.* 2010; Cheng *et al.* 2014). Fat-soluble micronutrients display large variations with regards to their solubility in mixed micelles (Sy *et al.* 2012; Gleize *et al.* 2016) and several factors are assumed to account for these differences (Desmarchelier & Borel 2017, for review).

The mixed micelle lipid composition has been shown to significantly affect vitamin absorption. For example, the substitution of lysophospholipids by phospholipids diminished the lymphatic absorption of vitamin E in rats (Koo *et al.* 2001). In rat perfused intestine, the addition of fatty acids of varying chain length and saturation degree, i.e. butyric, octanoic, oleic and linoleic acid, resulted in a decrease in the rate of D_3 absorption (Hollander *et al.* 1978). The effect was more pronounced in the ileal part of the small intestine following the addition of oleic and linoleic acid. It was suggested that unlike short- and medium-chain fatty acids, which are not incorporated into micelles, long-chain fatty acids hinder vitamin D absorption by causing enlargement of micelle size, thereby slowing their diffusion towards the enterocyte. Moreover, the possibility that D_3 could form self-aggregates in water (Meredith *et al.* 1984), although not clearly demonstrated, has led to question the need of mixed micelles for its solubilization in the aqueous environment of the intestinal tract lumen (Rautureau and Rambaud 1981; Maislos and Shany 1987).

This study was designed to compare the relative solubility of D_3 and RP in the aqueous phase rich in mixed micelles that exists in the upper intestinal lumen during digestion, and to dissect, by surface tension and surface pressure measurements, the molecular interactions existing between these vitamins and the mixed micelle components that explain the different solubility of D_3 and RP in mixed micelles.

2. Materials and methods

2.1. Chemicals

2-oleoyl-1-palmitoyl-sn-glycero-3-phosphocholine (POPC) (phosphatidylcholine, ≥99%; Mw 760.08 g/mol), 1-palmitoyl-sn-glycero-3-phosphocholine (Lyso-PC) (lysophosphatidylcholine, ≥99%; Mw 495.63 g/mol), free cholesterol (≥99%; Mw 386.65 g/mol), oleic acid (reagent grade, ≥99%; Mw 282.46 g/mol), 1-monooleoyl-*rac*-glycerol (monoolein, C18:1,-cis-9, Mw 356.54 g/mol), taurocholic acid sodium salt hydrate (NaTC) (≥95%; Mw 537.68 g/mol)), cholecalciferol (>98%; Mw 384.64 g/mol; melting point 84.5°C; solubility in water: 10^{-4}-10^{-5} mg/mL; logP 7.5) and retinyl palmitate (>93.5%; Mw 524.86 g/mol; melting point 28.5°C; logP 13.6) were purchased from Sigma-Aldrich (Saint-Quentin-Fallavier, France). Chloroform and methanol (99% pure) were analytical grade reagents from Merck (Germany). Ethanol (99.9%), n-hexane, chloroform, acetonitrile, dichloromethane and methanol were HPLC grade reagents from Carlo Erba Reagent (Peypin, France). Ultrapure water was produced by a Milli-Q® Direct 8 Water Purification System (Millipore, Molsheim, France). Prior to all surface tension, and surface pressure experiments, all glassware was soaked for an hour in a freshly prepared hot TFD4 (Franklab, Guyancourt, France) detergent solution (15% v/v), and then thoroughly rinsed with ultrapure water. Physico-chemical properties of D_3 and RP were retrieved from PubChem (https://pubchem.ncbi.nlm.nih.gov/).

125 *2.2. Micelle formation*

126 The micellar mixture contained 0.3 mM monoolein, 0.5 mM oleic acid, 0.04 mM POPC,
127 0.1 mM cholesterol, 0.16 mM Lyso-PC, and 5 mM NaTC (Reboul *et al.* 2005). Total component
128 concentration was thus 6.1 mM, with NaTC amounting to 82 mol%. Two vitamins were studied:
129 crystalline D_3 and RP.

130 Mixed micelles were formed according to the protocol described by Desmarchelier *et al.*
131 (2013). Lipid digestion products (LDP) (monoolein, oleic acid, POPC, cholesterol and Lyso-
132 PC, total concentration 1.1 mM) dissolved in chloroform/methanol (2:1, v/v), and D_3 or RP
133 dissolved in ethanol were transferred to a glass tube and the solvent mixture was carefully
134 evaporated under nitrogen. The dried residue was dispersed in Tris buffer (Tris-HCl 1mM,
135 $CaCl_2$ 5mM, NaCl 100 mM, pH 6.0) containing 5 mM taurocholate, and incubated at 37 °C for
136 30 min. The solution was then vigorously mixed by sonication at 25 W (Branson 250W sonifier;
137 Danbury, CT, U.S.A.) for 2 min, and incubated at 37 °C for 1 hour. To determine the amount
138 of vitamin solubilized in structures allowing their subsequent absorption by enterocytes
139 (bioaccessible fraction), *i.e.* micelles and possibly small lipid vesicles, whose size is smaller
140 than that of mucus pores (Cone 2009), the solutions were filtered through cellulose ester
141 membranes (0.22 μm) (Millipore), according to Tyssandier *et al.* 2003. The resulting optically
142 clear solution was stored at -20 °C until vitamin extraction and HPLC analysis. D_3 and RP
143 concentrations were measured by HPLC before and after filtration. For surface tension
144 measurements and cryoTEM experiments, the mixed micelle systems were not filtered.

145

146 *2.3. Self-micellarization of D_3*

147 Molecular assemblies of D_3 were prepared in Tris buffer using the same protocol as for
148 mixed micelles. D_3 was dissolved into the solvent mixture and after evaporation, the dry film
149 was hydrated for 30 min at 37°C with taurocholate-free buffer. The suspension was then

sonicated. All D_3 concentrations reported in the surface tension measurements were obtained from independent micellarization experiments - not from the dilution of one concentrated D_3 solution.

2.4. Surface tension measurements

Mixed micelle solutions were prepared as described above, at concentrations ranging from 5.5 nM to 55 mM, with the same proportion of components as previously mentioned. The surface tension of LDP mixtures hydrated with a taurocholate-free buffer, and that of pure taurocholate solutions were also measured at various concentrations. The solutions were poured into glass cuvettes. The aqueous surface was cleaned by suction, and the solutions were left at rest under saturated vapor pressure for 24 hours before measurements. For penetration studies, glass cuvettes with a side arm were used, allowing injection of NaTC beneath a spread LDP or vitamin monolayer. Surface tension measurements were performed by the Wilhelmy plate method, using a thermostated automatic digital tensiometer (K10 Krüss, Germany). The surface tension γ was recorded continuously as a function of time until equilibrium was reached. All experiments were performed at 25 ±1°C under saturated vapor pressure to maintain a constant level of liquid. The reported values are mean of three measurements. The experimental uncertainty was estimated to be 0.2 mN/m. Surface pressure (π) values were deduced from the relationship $\pi = \gamma_0 - \gamma$, with γ_0 the surface tension of the subphase and γ the surface tension in the presence of a film.

2.5. Surface pressure measurements

Surface pressure-area π-A isotherms of the LDP and LDP-vitamin mixtures were obtained using a thermostated Langmuir film trough (775.75 cm^2, Biolin Scientific, Finland) enclosed into a Plexiglas box (Essaid *et al.* 2016). Solutions of lipids in a chloroform/methanol

175 (9:1, v/v) mixture were spread onto a clean buffer subphase. Monolayers were left at rest for 20
176 minutes to allow complete evaporation of the solvents. They were then compressed at low speed
177 (6.5 $Å^2$.molecule^{-1}.min^{-1}) to minimize the occurrence of metastable phases. The experimental
178 uncertainty was estimated to be 0.1 mN/m. All experiments were run at 25 ±1°C. Mean
179 isotherms were deduced from at least three compression isotherms. The surface compressional
180 moduli K of monolayers were calculated using Eq. 1:

181 $$K = -A\left(\frac{d\pi}{dA}\right)_T \quad \text{(Eq. 1)}$$

182 Excess free energies of mixing were calculated according to Eq. 2:

183 $$\Delta G^{EXC} = \int_0^{\pi} \left(X_L A_L + X_{VIT} A_{VIT}\right) d\pi \quad \text{(Eq. 2)}$$

184 with X_L and A_L the molar fraction and molecular area of lipid molecules, and X_{VIT} and A_{VIT} the
185 molar fraction and molecular area of vitamin molecules, respectively (Ambike *et al.* 2011).

186

187 *2.6. Cryo-TEM analysis*

188 A drop (5 μL) of LDP-NaTC micellar solution (15 mM), LDP-NaTC-D_3 (3:1 molar ratio) or
189 pure D_3 "micellar suspension" (5 mM, theoretical concentration) was deposited onto a
190 perforated carbon-coated, copper grid (TedPella, Inc); the excess of liquid was blotted with a
191 filter paper. The grid was immediately plunged into a liquid ethane bath cooled with liquid
192 nitrogen (180 °C) and then mounted on a cryo holder (Da Cunha *et al*. 2016). Transmission
193 electron measurements (TEM) measurements were performed just after grid preparation using
194 a JEOL 2200FS (JEOL USA, Inc., Peabody, MA, U.S.A.) working under an acceleration
195 voltage of 200 kV (Institut Curie). Electron micrographs were recorded by a CCD camera
196 (Gatan, Evry, France).

197

198 *2.7. Vitamin analysis*

199 2.7.1. Vitamin extraction.

200 D_3 and RP were extracted from 500 µL aqueous samples using the following method
201 (Desmarchelier *et al.* 2013): retinyl acetate was used as an internal standard and was added to
202 the samples in 500 µL ethanol. The mixture was extracted twice with two volumes of hexane.
203 The hexane phases obtained after centrifugation (1200 × g, 10 min, 10°C) were evaporated to
204 dryness under nitrogen, and the dried extract was dissolved in 200 µL of
205 acetonitrile/dichloromethane/methanol (70:20:10, v/v/v). A volume of 150 µL was used for
206 HPLC analysis. Extraction efficiency was between 75 and 100%. Sample whose extraction
207 efficiency was below 75% were re-extracted or taken out from the analysis.

208

209 2.7.2. Vitamin HPLC analysis.

210 D_3, and RP and retinyl acetate were separated using a 250 x 4.6-nm RP C18, 5-µm Zorbax
211 Eclipse XDB column (Agilent Technologies, Les Ulis, France) and a guard column. The mobile
212 phase was a mixture of acetonitrile/dichloromethane/methanol (70:20:10, v/v/v). Flow rate was
213 1.8 mL/min and the column was kept at a constant temperature (35 °C). The HPLC system
214 comprised a Dionex separation module (P680 HPLC pump and ASI-100 automated sample
215 injector, Dionex, Aix-en-Provence, France). D_3 was detected at 265 nm while retinyl esters
216 were detected at 325 nm and were identified by retention time compared with pure (>95%)
217 standards. Quantification was performed using Chromeleon software (version 6.50, SP4 Build
218 1000) comparing the peak area with standard reference curves. All solvents used were HPLC
219 grade.

220

221 *2.8. Statistical analysis*

Results are expressed as means ± standard deviation. Statistical analyses were performed using Statview software version 5.0 (SAS Institute, Cary, NC, U.S.A.). Means were compared by the non-parametric Kruskal-Wallis test, followed by Mann-Whitney U test as a post hoc test for pairwise comparisons, when the mean difference using the Kruskal-Wallis test was found to be significant ($P<0.05$). For all tests, the bilateral alpha risk was $\alpha = 0.05$.

3. Results

3.1. Solubilization of D_3 and RP in aqueous solutions rich in mixed micelles

D_3 and RP at various concentrations were mixed with micelle components (LDP-NaTC). D_3 and RP concentrations were measured by HPLC before and after filtration of aggregates with a diameter smaller than 0.22 µm (Figure 2). D_3 and RP solubilization in the solution that contained mixed micelle solution followed different curves: D_3 solubilization was linear (R^2=0.98, regression slope = 0.71) and significantly higher than that of RP, which reached a plateau with a maximum concentration around 125 µM.

The morphology of the LDP-NaTC and LDP-NaTC-D_3 samples before filtration was analyzed by cryoTEM. In Figure 3, micelles are too small to be distinguished from ice. At high LDP-NaTC concentration (15 mM) small and large unilamellar vesicles (*a*), nano-fibers (*b*) and aggregates (*c*) are observed (Figure 3A). Both nano-fibers and aggregates seem to emerge from the vesicles. In the presence of D_3 at low micelle and D3 concentration (5 mM LDP-NaTC + 1.7 mM D_3) (Figures 3B and 3C), the morphology of the nano-assemblies is greatly modified. Vesicles are smaller and deformed, with irregular and more angular shapes (*a'*). There are also more abundant. A difference in contrast in the bilayers is observed, which would account for leaflets with asymmetric composition. Some of them coalesce into larger structures, extending along the walls of the grid (*d*). Fragments and sheets are also observed (figure 3B). They exhibit

247 irregular contour and unidentified membrane organization. The bilayer structure is not clearly
248 observable. New organized assemblies appear, such as disk-like nano-assemblies (*e*) and
249 emulsion-like droplets (*f*). At higher concentration (15 mM LDP-NaTC + 5 mM D_3 in figure
250 3D), the emulsion-like droplets and vesicles with unidentified membrane structure (*g*) are
251 enlarged. They coexist with small deformed vesicules.
252
253 *3.2. Compression properties of LDP components, the LDP mixture and the vitamins*
254 To better understand the mechanism of D_3 and RP interaction with LDP-NaTC micelles,
255 we focused on the interfacial behavior of the various components of the system. We first
256 determined the interfacial behavior of the LDP components and their mixture in proportions
257 similar to those in the micellar solution, by surface pressure measurements. The π-A isotherms
258 are plotted in Figure 4A. Based on the calculated compressibility modulus values, the lipid
259 monolayers can be classified into poorly organized ($K < 100$ mN/m, for lyso-PC, monoolein,
260 and oleic acid), liquid condensed ($100 < K < 250$ mN/m, for POPC and the LDP mixture) and
261 highly rigid monolayers ($K > 250$ mN/m, for cholesterol) (Davies & Rideal 1963).
262 The interfacial behavior of the two studied vitamins is illustrated in Figure 4B. D_3 shows
263 a similar compression profile to that of the LDP mixture, with comparable surface area and
264 surface pressure at collapse ($A_c = 35$ Å^2, $\pi_c = 38$ mN/m) but a much higher rigidity, as inferred
265 from the comparison of their maximal K values (187.4 mN/m and 115.4 mN/m for D_3 and LDP,
266 respectively). RP exhibits much larger surface areas and lower surface pressures than D_3. The
267 collapse of its monolayer is not clearly identified from the isotherms, and is estimated to occur
268 at $\pi_c = 16.2$ mN/m ($A_c = 56.0$ Å^2), as deduced from the slope change in the π-A plot.
269
270 *3.3. Self-assembling properties of D_3 in an aqueous solution*

Since D_3 showed an interfacial behavior similar to that of the lipid mixture, and since it could be solubilized at very high concentrations in an aqueous phase rich in mixed micelles (as shown in Figure 2), its self-assembling properties were more specifically investigated. Dried D_3 films were hydrated with the sodium taurocholate free-buffer. Surface tension measurements at various D_3 concentrations revealed that the vitamin could adsorb at the air/solution interface, and significantly lower the surface tension of the buffer to γ_{cmc} = 30.6 mN/m. A critical micellar concentration (cmc = 0.45 μM) could be deduced from the γ-log C relationships and HPLC assays. Concentrated samples D_3 samples were analyzed by cryo-TEM (Figure 3E and 3F). Different D_3 self-assemblies were observed, including circular nano-assemblies (*h*) coexisting with nano-fibers (*i*), and large aggregates (*j*) with unidentified structure. The analysis in depth of the circular nano-assemblies allowed to conclude that they were disk-like nano-assemblies, rather than nanoparticles.

3.4. Interaction of LDP with NaTC

To better understand how the two studied vitamins interacted with the mixed micelles, we compared the interfacial behaviors of the pure NaTC solutions, LDP mixtures hydrated by NaTC-free buffer, and LDP mixtures hydrated by the NaTC buffered solutions (full mixed micelle composition). The LDP mixture composition was maintained constant, while its concentration in the aqueous medium was increased. The concentration of NaTC in the aqueous phase was also calculated so that the relative proportion of the various components (LDP and NaTC) remained unchanged in all experiments. From the results plotted in Figure 5A, the critical micellar concentration (cmc) of the LDP-NaTC mixture was 0.122 mM (γ_{cmc} = 29.0 mN/m), a concentration 50.8 times lower than the concentration used for vitamin solubilization. The cmc values for the LDP mixture and the pure NaTC solutions were 0.025 mM (γ_{cmc} = 24.0 mN/m), and 1.5 mM (γ_{cmc} = 45.3 mN/m), respectively.

296 Experiments modeling the insertion of NaTC into the LDP film during rehydration by
297 the buffer suggested that only few NaTC molecules could penetrate in the condensed LDP film
298 (initial surface pressure: π_i = 28 mN/m) and that the LDP-NaTC mixed film was not stable, as
299 shown by the decrease in surface pressure over time (Figure 5B).
300
301 *3.5. Interaction of D_3 and RP with NaTC*
302 The surface tension of the mixed NaTC-LDP micelle solutions was only barely affected
303 by the addition of 0.1 or 1 mM D_3 or RP: the surface tension values increased by no more than
304 2.8 mN/m. Conversely, both vitamins strongly affected the interfacial behavior of the NaTC
305 micellar solution, as inferred from the significant surface tension lowering observed (- 7.0 and
306 - 8.1 mN/m for RP and D_3, respectively).
307
308 *3.6. Interaction of D_3 and RP with lipid digestion products*
309 The interaction between the vitamins and LDP molecules following their insertion into
310 LDP micelles was modeled by compression of LDP/D_3 and LDP/RP mixtures at a 7:3 molar
311 ratio. This ratio was chosen arbitrarily, to model a system in which LDP was in excess. The π-
312 A isotherms are presented in Figures 6A and 6B. They show that both vitamins modified the
313 isotherm profile of the lipid mixture, however, not in the same way. In the LDP/D_3 mixture, the
314 surface pressure and molecular area at collapse were controlled by LDP. For LDP/RP, despite
315 the high content in LDP, the interfacial behavior was clearly controlled by RP. From the
316 isotherms in Figures 6A and 6B, compressibility moduli and excess free energies of mixing
317 were calculated and compared (Figures 6C, and 6D). D_3 increased the rigidity of LDP
318 monolayers, whereas RP disorganized them. The negative ΔG^{EXC} values calculated for the LDP-
319 D_3 monolayers at all surface pressures account for the good mixing properties of D_3 and the

lipids in all molecular packing conditions. Conversely for RP, the positive and increasing ΔG^{EXC} values with the surface pressure demonstrate that its interaction with the lipids was unfavorable.

4. Discussion

The objective of this study was to compare the solubility of RP and D_3 in aqueous solutions containing mixed micelles, and to decipher the molecular interactions that explain their different extent of solubilization. Our first experiment revealed that the two vitamins exhibit very different solubilities in an aqueous medium rich in mixed micelles. Furthermore, the solubility of D_3 was so high that we did not observe any limit, even when D_3 was introduced at a concentration > 1mM in the aqueous medium. To our knowledge, this is the first time that such a difference is reported. Cryo-TEM pictures showed that D_3 dramatically altered the organization of the various components of the mixed micelles. The spherical vesicles were deformed with angular shapes. The nano-fibers initiating from the vesicles were no longer observed. Large irregular in shape vesicle and sheets, disk-like nano-assemblies and emulsion-like droplets appeared in LDP-NaTC-D_3 mixtures, only. The existence of so many different assemblies would account for a different interaction of D_3 with the various components of mixed micelles, and for a reorganization of the components. D_3 could insert in the bilayer of vesicles and deform them, but also form emulsion-like droplets with fatty acids and monoglyceride. It is noteworthy that these emulsion-like droplets were not observed in pure D_3 samples, nor mixed micelles. Since previous studies have shown that both bile salts and some mixed micelle lipids, e.g. fatty acids and phospholipids, can modulate the solubility of fat-soluble vitamins in these vehicles (Yang & McClements 2013), we decided to study the

342 interactions of these two vitamins with either bile salts or micelle lipids to assess the specific
343 role of each component on vitamin solubility in mixed micelles.

344 The characteristics of pure POPC, Lyso-PC, monoolein, and cholesterol isotherms were
345 in agreement with values published in the literature (Pezron *et al.* 1991; Flasinsky *et al.* 2014;
346 Huynh *et al.* 2014). For oleic acid, the surface pressure at collapse was higher (π_c = 37 mN/m)
347 and the corresponding molecular area (A_c = 26 $Å^2$) smaller than those previously published
348 (Tomoaia-Cotisel *et al*. 1987), likely due to the pH of the buffer solution (pH 6) and the presence
349 of calcium.

350 The interfacial properties of D_3 were close to those deduced from the isotherm published
351 by Meredith *et al.* (1984) for a D_3 monolayer spread from a benzene solution onto a pure water
352 subphase. The molecular areas at collapse are almost identical in the two studies (about 36 $Å^2$),
353 but the surface pressures differ (30 mN/m in Meredith and coworkers' study, and 38 mN/m in
354 ours). Compressibility modulus values show that D_3 molecules form monolayers with higher
355 molecular order than the LDP mixture, which suggests that they might easily insert into LDP
356 domains.

357 As could be expected from its chemical structure, RP exhibited a completely different
358 interfacial behavior compared to D_3 and the LDP, even to lyso-PC which formed the most
359 expanded monolayers of the series, and displayed the lowest collapse surface pressure. The
360 anomalous isotherm profile of lyso-PC has been attributed to monolayer instability and
361 progressive solubilization of molecules into the aqueous phase (Heffner *et al.* 2013). The
362 molecular areas and surface pressures for RP have been compared to those measured by Asai
363 and Watanabe (2000) for RP monolayers spread from benzene solutions at 25°C onto a water
364 subphase. Their values are much lower than ours, accounting for even more poorly organized
365 monolayers. The low collapse surface pressure could correspond to molecules partially lying
366 onto the aqueous surface, possibly forming multilayers above 16 mN/m as inferred from the

continuous increase in surface pressure above the change in slope of the isotherm. The maximal compressibility modulus confirms the poor monolayer order. The significant differences in RP surface pressure and surface area compared to the LDP mixture might compromise its insertion and stability into LDP domains.

The dogma in nutrition is that fat-soluble vitamins need to be solubilized in bile salt micelles to be transported to the enterocyte and then absorbed. It is also well known that although NaTC primary micelles can be formed at 2-3 mM with a small aggregation number, concentrations as high as 10-12 mM are usually necessary for efficient lipid solubilization in the intestine (Baskin & Frost 2008). Due to their chemical structure bile salts have a facial arrangement of polar and non-polar domains (Madency & Egelhaaf 2010). Their self-assembling (dimers, multimers, micelles) is a complex process involving hydrophobic interaction and cooperative hydrogen bonding, highly dependent on the medium conditions, and that is not completely elucidated. The cmc value for sodium taurocholate in the studied buffer was particularly low compared to some of those reported in the literature for NaTC in water or sodium chloride solutions (3-12 mM) (Kratohvil *et al.* 1983; Meyerhoffer & Mcgown 1990; Madenci & Egelhaaf 2010). At concentrations as high as 10-12 mM, NaTC molecules form elongated cylindrical "secondary" micelles (Madenci & Egelhaaf 2010; Bottari *et al.* 1999). The cryoTEM analysis did not allow to distinguish micelles from the ice. In our solubilization experiment, the concentration of NaTC did not exceed 5 mM. Nevertheless, the micelles proved to be very efficient with regards to vitamin solubilization.

When bile salts and lipids are simultaneously present in the same environment, they form mixed micelles (Hernell *et al.* 1990). Bile salts solubilize phospholipid vesicles and transform into cylindrical micelles (Cheng *et al.* 2014). Walter et al (1991) suggested that sodium cholate cylindrical micelles evolved from the edge of lecithin bilayer sheets. Most published studies were performed at high phospholipid/bile salt ratio. In our system, the

concentration of the phospholipids was very low compared to that of NaTC. We observed however the presence of vesicles, and nano-fiber structures emerging from them. In their cryoTEM analysis, Fatouros *et al*. (2009) compared bile salt/phospholipid mixtures to bile salt/phospholipid/fatty acid/monoglyceride ones at concentrations closer to ours. They observed only micelles in bile salt/phospholipid mixtures. However, in the presence of oleic acid and monoolein, vesicles and bilayer sheets were formed. This would account for a reorganization of the lipids and bile salts in the presence of the fatty acid and the monoglyceride. We therefore decided to study the interactions between bile salts and LDP. The results obtained show that the surface tension, the effective surface tension lowering concentration, and cmc values were very much influenced by LDP. The almost parallel slopes of Gibbs adsorption isotherms for pure NaTC and mixed NaTC-LDP suggest that LDP molecules inserted into NaTC domains, rather than the opposite. This was confirmed by penetration studies, which showed that NaTC (0.1 mM) could hardly penetrate in a compact LDP film. So, during lipid hydration, LDP molecules could insert into NaTC domains. The presence of LDP molecules improved NaTC micellarization.

After having determined the interfacial properties of each micelle component and measured the interactions between NaTC and LDP, we assessed the ability of D_3 and RP to solubilize in either NaTC or NaTC-LDP micelles. Surface tension values clearly show that both vitamins could insert in between NaTC molecules adsorbed at the interface, and affected the surface tension in the same way. The interfacial behavior of the molecules being representative of their behavior in the bulk, it is reasonable to think that both D_3 and RP can be solubilized into pure NaTC micelles. For the mixed NaTC-LDP micelles, the change in surface tension was too limited to allow conclusions, but the solubilization experiments clearly indicated that neither vitamin was solubilized to the same extent.

Solubilization experiments and the analysis of vitamin-NaTC interaction cannot explain why the LDP-NaTC mixed micelles solubilize D_3 better than RP. Therefore, we studied the interfacial behavior of the LDP mixture in the presence of each vitamin, to determine the extent of their interaction with the lipids. The results obtained showed that D_3 penetrated in LDP domains and remained in the lipid monolayer throughout compression. At large molecular areas, the π-A isotherm profile of the mixture followed that of the LDP isotherm with a slight condensation due to the presence of D_3 molecules. Above 10 mN/m, an enlargement of the molecular area at collapse and a change in the slope of the mixed monolayer was observed. However, the surface pressure at collapse was not modified, and the shape of the isotherm accounted for the insertion of D_3 molecules into LDP domains. This was confirmed by the surface compressional moduli. D_3 interacted with lipid molecules in such manner that it increased monolayer rigidity (K_{max} = 134.8 mN/m), without changing the general organization of the LDP monolayer. The LDP-D_3 mixed monolayer thus appeared more structured than the LDP one. D_3 behavior resembles that of cholesterol in phospholipid monolayers, however without the condensing effect of the sterol (Ambike *et al.* 2011). The higher rigidity of LDP monolayer in the presence of D_3 could be related to the cryo-TEM pictures showing the deformed, more angular vesicles formed with LDP-NaTC-D_3. The angular shape would account for vesicles with rigid bilayers (Kuntsche *et al.* 2011).

For RP, the shape of the isotherms show evidence that lipid molecules penetrated in RP domains, rather than the opposite. Indeed, the π-A isotherm profile of the LDP-RP monolayer is similar to that of RP alone. The insertion of lipid molecules into RP domains is also attested by the increase in the collapse surface pressure from 16 to 22 mN/m. Partial collapse is confirmed by the decrease in the compressibility modulus above 22 mN/m. Thus, RP led to a destructuration of the LDP mixed monolayer and when the surface density of the monolayer increased, the vitamin was partially squeezed out from the interface. The calculated ΔG^{EXC}

441 values for both systems suggest that insertion of D_3 into LDP domains was controlled by
442 favorable (attractive) interactions, whereas mixing of RP with LDP was limited due to
443 unfavorable (repulsive) interactions, even at low surface pressures. According to Asai and
444 Watanabe (2000), RP can be partially solubilized in the bilayer of phospholipids (up to 3
445 mol%), and the excess is separated from the phospholipids, and dispersed as emulsion droplets
446 stabilized by a phospholipid monolayer.

447 On the whole, the information obtained regarding the interactions of the two vitamins
448 with NaTC and LDP explain why D_3 is more soluble than RP in an aqueous medium rich in
449 mixed micelles. Both vitamins can insert into pure NaTC domains, but only D_3 can also insert
450 into the LDP domains in LDP-enriched NaTC micelles.

451 Furthermore, the results obtained suggest that this is not the only explanation. Indeed,
452 since it has been suggested that D_3 could form cylindrical micelle-like aggregates (Meredith *et*
453 *al.* 1984), we hypothesize that the very high solubility of D_3 in the aqueous medium rich in
454 mixed micelles was partly due to the solubilization of a fraction of D_3 as self-aggregates. Indeed,
455 we observed that D_3 at concentrations higher than 0.45 µM, could self-assemble into various
456 structures including nano-fibers. To our knowledge, no such structures, especially nanofibers,
457 have been reported for D_3 so far. Rod diameter was smaller than 10 nm, much smaller than for
458 the rods formed by lithocholic acid, for example (Terech *et al.* 2002). They were similar to
459 those observed in highly concentrated LDP-NaTC mixtures, which seemed formed *via*
460 desorganization of lipid vesicles. Disk-like and aggregates with unidentified structure, also
461 observed in concentrated D_3 samples, could be related to these nano-fibers.

462 In our solubilization experiments, which were performed at much higher D_3
463 concentrations, both insertion of D_3 molecules into NaTC and LDP domains, and D_3 self-

assembling could occur, depending on the kinetics of insertion of D_3 into the NaTC-DLP mixed micelles.

5. Conclusion

The solubilization of a hydrophobic compound in bile salt-lipid micelles is dependent upon its chemical structure and its ability to interact with the mixed micelles components. Most hydrophobic compounds are expected to insert into the bile salt-lipid micelles. The extent of the solubilizing effect is, however, much more difficult to predict. As shown by others before us, mixed micelles components form a heterogeneous system with various molecular assemblies differing in shape and composition. The conditions of the medium (pH, ionic strength and temperature) affect the formation of these molecular assemblies, although we did not study this effect on our system. Our results showed that D_3 displayed a higher solubility in mixed micelle solutions than RP. This difference was attributed to the different abilities of the two vitamins to insert in between micelle components, but it was also explained by the propensity of D_3, contrarily to RP, to self-associate into structures that are readily soluble in the aqueous phase. It is difficult to predict the propensity of a compound to self-association. We propose here a methodology that was efficient to distinguish between two solubilizing behaviors, and could be easily used to predict the solubilization efficiency of other hydrophobic compounds. Whether the D_3 self-assemblies are available for absorption by the intestinal cells needs further studies.

Acknowledgements: The authors are grateful to Dr Sylvain Trépout (Institut Curie, Orsay, France) for his contribution to cryoTEM experiments and the fruitful discussions.

Funding: This study was funded by Adisseo France SAS.

Conflicts of interest: DP, ED and VLD are employed by Adisseo. Adisseo markets formulated vitamins for animal nutrition.

References

Ambike, A., Rosilio, V., Stella, B., Lepetre-Mouelhi, S., & Couvreur, P. (2011) Interaction of self-assembled squalenoyl gemcitabine nanoparticles with phospholipid-cholesterol monolayers mimicking a biomembrane. *Langmuir, 27*, 4891-4899.

Asai, Y., & Watanabe, S. (2000) Formation and stability of the dispersed particles composed of retinyl palmitate and phosphatidylcholine. *Pharmaceutical Development and Technology, 5*, 39-45.

Baskin, R., & Frost, L. D. (2008) Bile salt-phospholipid aggregation at submicellar concentrations. *Colloids and Surface B: Biointerfaces, 62*, 238-242.

Bottari, E., D'Archivio, A. A., Festa, M. R., Galantini, L., & Giglio, E. (1999) Structure and composition of sodium taurocholate micellar aggregates. *Langmuir, 15*, 2996-2998.

Borel, P., Caillaud, D., & Cano, N. J. (2015) Vitamin D bioavailability: state of the art. *Critical Reviews in Food Science and Nutrition, 55*, 1193-1205.

Borel, P., & Desmarchelier, C. (2017) Genetic Variations Associated with Vitamin A Status and Vitamin A Bioavailability. *Nutrients, 9,* 246.

515 Cheng, C.-Y., Oh, H., Wang, T.-Y., Ragavan, S.R. & Tung, S.-H. (2014) Mixtures of lecithin
516 and bile salt can form highly viscous wormlike micellar solutions in water. *Langmuir, 30,*
517 10221-10230.

518

519 Cone, R.A. (2009) Barrier properties of mucus. *Advanced drug delivery reviews, 61*, 75-85.

520

521 Da Cunha, M. M., Trepout, S., Messaoudi, C., Wu, T. D., Ortega, R., Guerquin-Kern, J. L., &
522 Marco, S. (2016) Overview of chemical imaging methods to address biological questions.
523 *Micron, 84*, 23-36.

524

525 Davies, J. T., & Rideal, E. K. (1963) Interfacial phenomena 2nd ed. Academic press, p. 265.

526

527 Desmarchelier, C., Tourniaire, F., Preveraud, D. P., Samson-Kremser, C., Crenon, I., Rosilio,
528 V., & Borel, P. (2013) The distribution and relative hydrolysis of tocopheryl acetate in the
529 different matrices coexisting in the lumen of the small intestine during digestion could explain
530 its low bioavailability. *Molecular Nutrition and Food Research, 57*, 1237-1245.

531

532 Desmarchelier, C., Margier, M., Preveraud, D., Nowicki, M., Rosilio, V., Borel, P., & Reboul,
533 E. (2017) Comparison of the micellar incorporation and the uptake of cholecalciferol, 25-
534 hydroxycholecalciferol and 1-α-hydroxycholecalciferol by the intestinal cell, *Nutrients, 9,*
535 1152.

536

537 Desmarchelier, C., & Borel, P. (2017) Overview of carotenoid bioavailability determinants:
538 From dietary factors to host genetic variations. *Trends in Food Science & Technology, 69,* 270-
539 280.

540

541 Essaid, D., Rosilio, V., Daghildjian, K., Solgadi, A., Vergnaud, J., Kasselouri, A., &
542 Chaminade, P. (2016) *Biochimica Biophysica Acta, 1858,* 2725-2736.

543

Fatouros, D.G., Walrand, I., Bergenstahl, B., Müllertz, A. (2009) Colloidal structures in media simulating intestinal fed state conditions with and without lypolysis products. *Pharmaceutical Research, 26,* 361-374.

Flasinski, M., Wydro, P., & Broniatowski, M. (2014) Lyso-phosphatidylcholines in Langmuir monolayers-influence of chain length on physicochemical characteristics of single-chained lipids. *Journal of Colloid and Interface Science, 418*, 20-30.

Gleize, B., Nowicki, M., Daval, C., Koutnikova, H., and Borel, P. (2016) Form of phytosterols and food matrix in which they are incorporated modulate their incorporation into mixed micelles and impact cholesterol micellarization. *Molecular Nutrition and Food Research, 60*, 749-759

Heffner, C. T. R., Pocivavsek, L., Birukova, A. A., Moldobaeva, N., Bochkov, V. N., Lee, K. Y. C., & Birukov, K. G. (2013) Thermodynamic and kinetic investigations of the release of oxidized phospholipids from lipid membranes and its effect on vascular integrity. *Chemistry and Physics of lipids 175-176,* 9-19.

Hernell, O., Staggers, J. E., & Carey, M. C. (1990) Physical-chemical behavior of dietary and biliary lipids during intestinal digestion and absorption. 2. Phase analysis and aggregation states of luminal lipids during duodenal fat digestion in healthy adult human beings. *Biochemistry, 29,* 2041-2056.

Hollander, D., Muralidhara, K. S., & Zimmerman, A. (1978) Vitamin D-3 intestinal absorption in vivo: influence of fatty acids, bile salts, and perfusate pH on absorption. *Gut, 19*, 267-272.

Huynh, L., Perrot, N., Beswick, V., Rosilio, V., Curmi, P. A., Sanson, A., & Jamin, N. (2014) Structural properties of POPC monolayers under lateral compression: computer simulations analysis. *Langmuir, 30*, 564-573.

574 Koo, S. I., & Noh, S. K. (2001) Phosphatidylcholine inhibits and lysophosphatidylcholine
575 enhances the lymphatic absorption of alpha-tocopherol in adult rats. *Journal of Nutrition, 131*,
576 717-722.

577

578 Kratohvil, J. P., Hsu, W. P., Jacobs, M. A., Aminabhavi, T. M., & Mukunoki, Y. (1983)
579 Concentration-dependent aggregation patterns of conjugated bile-salts in aqueous sodium-
580 chloride solutions - a comparison between sodium taurodeoxycholate and sodium taurocholate.
581 *Colloid and Polymer Science, 261*, 781-785.

582

583 Kuntsche, J., Horst, J.C, & Bunjes, H., Cryogenic transmission electron microscopy (cryo-
584 TEM) for studying the morphology of collidal drug delivery systems (2011) *International*
585 *Journal of Pharmaceutics 417,* 120-137.

586

587 Leng, J., Egelhaaf, S.U., & Cates, M.E. (2003) Kinetics of the micelle-to-vesicle transition ;
588 aquous lecithin-bile salt mixtures, *Biophysical Journal*, 85, 1624-1646.

589

590 Madenci, D., & Egelhaaf, S. U. (2010) Self-assembly in aqueous bile salt solutions. *Current*
591 *Opinion in Colloid and Interface Science, 15*, 109-115.

592

593 Maislos, M., & Shany, S. (1987) Bile salt deficiency and the absorption of vitamin D
594 metabolites. In vivo study in the rat. *Israel Journal of Medical Sciences, 23*, 1114-1117

595

596 Meredith, S. C., Bolt, M. J., & Rosenberg, I. H. (1984) The Supramolecular Structure of
597 Vitamin-D3 in Water. *Journal of Colloid and Interface Science, 99*, 244-255.

598

599 Meyerhoffer, S. M., & Mcgown, L. B. (1990) Critical Micelle Concentration Behavior of
600 Sodium Taurocholate in Water. *Langmuir, 6*, 187-191.

601

602 Pezron, I., Pezron, E., Claesson, P. M., & Bergenstahl, B. A. (1991) Monoglyceride Surface-
603 Films - Stability and Interlayer Interactions. *Journal of Colloid and Interface Science,* **144**, 449-
604 457.

605

606 Rautureau, M., & Rambaud, J. C. (1981) Aqueous solubilisation of vitamin D3 in normal man.
607 *Gut, 22*, 393-397.

608

609 Reboul, E., Abou, L., Mikail, C., Ghiringhelli, O., Andre, M., Portugal, H., Jourdheuil-
610 Rahmani, D., Amiot, M. J., Lairon, D., & Borel, P. (2005) Lutein transport by Caco-2 TC-7
611 cells occurs partly by a facilitated process involving the scavenger receptor class B type I (SR-
612 BI). *Biochemical Journal, 387*, 455-461.

613

614 Reboul, E., & Borel, P. (2011) Proteins involved in uptake, intracellular transport and
615 basolateral secretion of fat-soluble vitamins and carotenoids by mammalian enterocytes.
616 *Progress in Lipid Research, 50*, 388-402.

617

618 Salentinig, S., Sagalowicz, L., & Glatter, O. (2010) Self-assembled structures and pKa value of
619 oleic acid in systems of biological relevance, *Langmuir 26,* 11670-11679.

620

621 Sy, C., Gleize, B., Dangles, O., Landrier, J. F., Veyrat, C. C., & Borel, P. (2012) Effects of
622 physicochemical properties of carotenoids on their bioaccessibility, intestinal cell uptake, and
623 blood and tissue concentrations. *Molecular Nutrition and Food Research,* **56**, 1385-1397.

624

625 Terech, P., de Geyer, A., Struth, B., & Talmon, Y. (2002) Self-assembled monodisperse steroid
626 nanotubes in water. *Advanced Materials, 14*, 495-498.

627

628 Tomoaia-Cotisel, M., Zsako, J., Mocanu, A., Lupea, M., & Chifu, E. (1987) Insoluble mixed
629 monolayers. *Journal of Colloid and Interface Science, 117*, 464-476.

630

631 Tyssandier, V., Reboul, E., Dumas, J.-F., Bouteloup-Demange, C., Armand, M., Marcand, J.,
632 Sallas, M., & Borel, P. (2003) Processing of vegetable-borne carotenoids in the human stomach
633 and duodenum. *American Journal of Physiology - Gastrointestinal and Liver Physiology, 284,*
634 G913-G923.
635
636 Walter, A., Vinson, P.K., Kaplun, A., & Talmon, Y. (1991) Intermediate structures in the
637 cholate-phosphatidylcholine vesicle-micelle transition, *Biophysical Journal, 60,* 1315-1325.
638
639 Yang, Y., & McClements, D. J. (2013) Vitamin E and vitamin E acetate solubilization in mixed
640 micelles: physicochemical basis of bioaccessibility. *Journal of Colloid and Interface Science,*
641 *405*, 312-321.
642
643

644 **Figure Captions**

645 **Figure 1:** Chemical structures for D_3 and RP.

646

647 **Figure 2:** Solubilization of D_3 and RP in aqueous solutions rich in mixed micelles: (●),
648 cholecalciferol; (□), retinyl palmitate. For D_3 $R^2 = 0.98$, and regression slope = 0.71.

649

650 **Figure 3:** Cryo-TEM morphology of (A) 15 mM mixed LDP-NaTC micelles, (B) and (C) 5
651 mM mixed LDP-NaTC micelles +1.7 mM D_3, (D) 15 mM mixed LDP-NaTC micelles + 5 mM
652 D_3, (E) and (F) pure D_3 assemblies: (*a*) spherical vesicles, (*a'*) small deformed vesicles, (*b*)
653 nano-fibers, (*c*) aggregates, (*d*) large deformed vesicle fragments (sheets), (*e*) disk-like nano-
654 assembly, (*f*) emulsion-like droplet, (*g*) large deformed vesicle, (*h*) disk-like nano-assemblies,
655 (*i*) nano-fibers, (*h*) aggregates. All samples were prepared by the dry film hydration method,
656 without filtration. Scale bars: 100 nm.

657

658 **Figure 4:** Mean compression isotherms for (A) the pure micelles components and the LDP
659 mixture, and (B) D_3 (solid line) and RP (dashed line) spread at the air/buffer interface from a
660 chloroform-methanol (9:1) solution (25°C). POPC (●), LysoPC (○), monoolein (△),
661 cholesterol (▲), oleic acid (□), LDP (dashed line).

662

663 **Figure 5:** (A) Adsorption isotherms for LDP hydrated in NaTC-free buffer (○), LDP hydrated
664 in NaTC-containing buffer solution (■), and pure NaTC (♦) solutions at 25°C. (B) Surface
665 pressure increment upon injection of NaTC beneath a condensed LDP monolayer (π_i = 28
666 mN/m). The final NaTC concentration in the subphase was 0.1 mM. The initial increase in
667 surface pressure following NaTC addition to the subphase was an injection effect.

668

669 **Figure 6:** π-A isotherms (A,B), compressibility moduli (C) and excess free energies (D) for
670 LDP-vitamin monolayers (25°C). A: LDP mixture (dashed line), pure D_3 (dashed-dot line) and
671 LDP-D_3 (7:3) mixture (solid line); B: LDP mixture (dashed line), RP (dashed-dot line) and
672 LDP-RP (7:3) mixture (solid line). C: LDP mixture (dashed line), LDP-D_3 (7:3) mixture (solid
673 line), and LDP-RP (7:3) mixture (dashed-dot-dot line). D: LDP-D_3 (7:3) (square) and LDP-RP
674 (7:3) (triangle) mixtures.

Figure 1

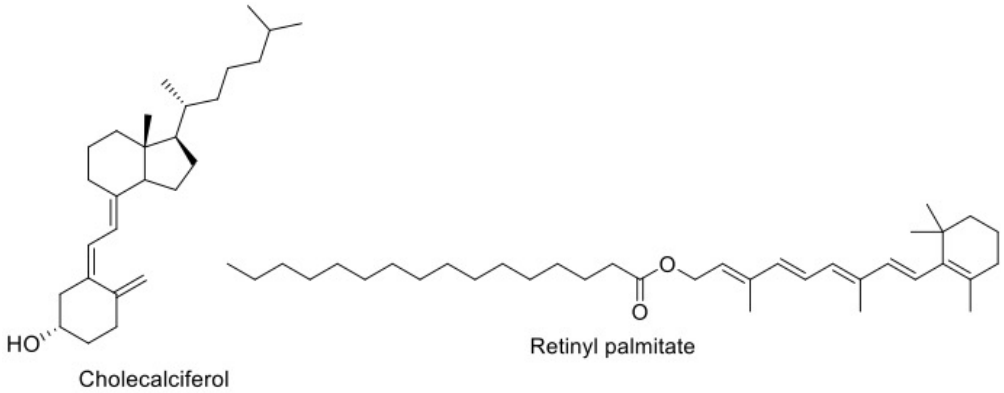

Figure 2

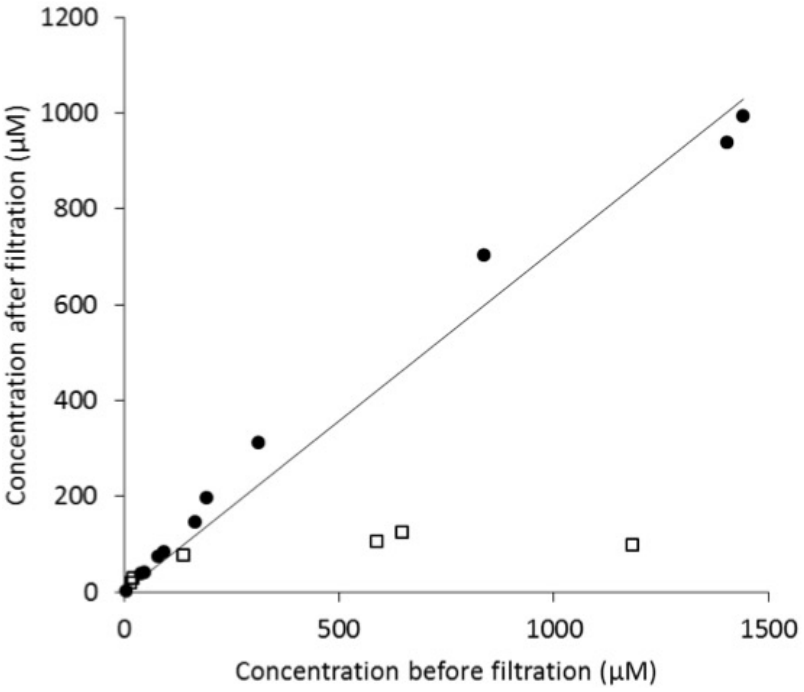

Figure 3

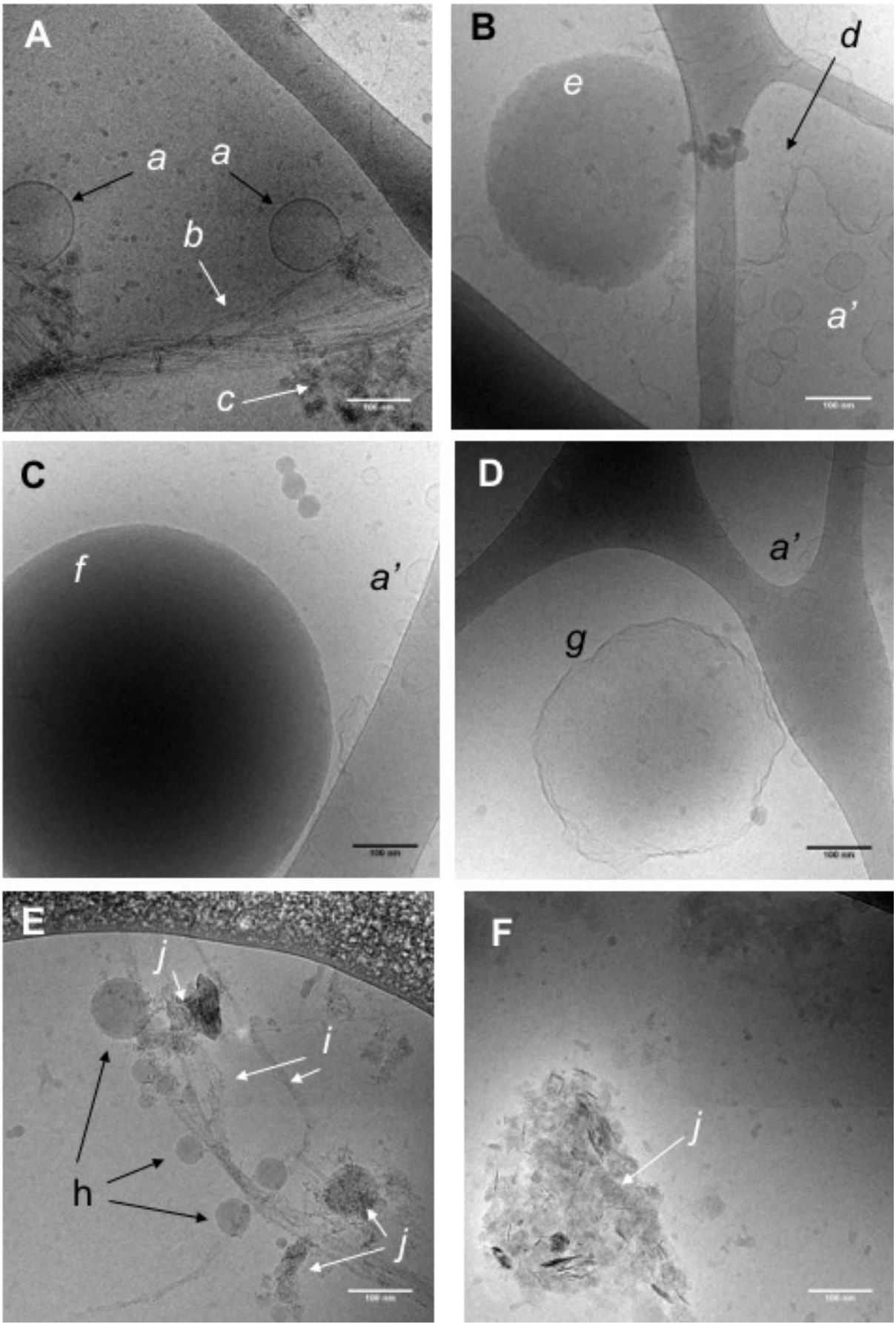

Figure 4

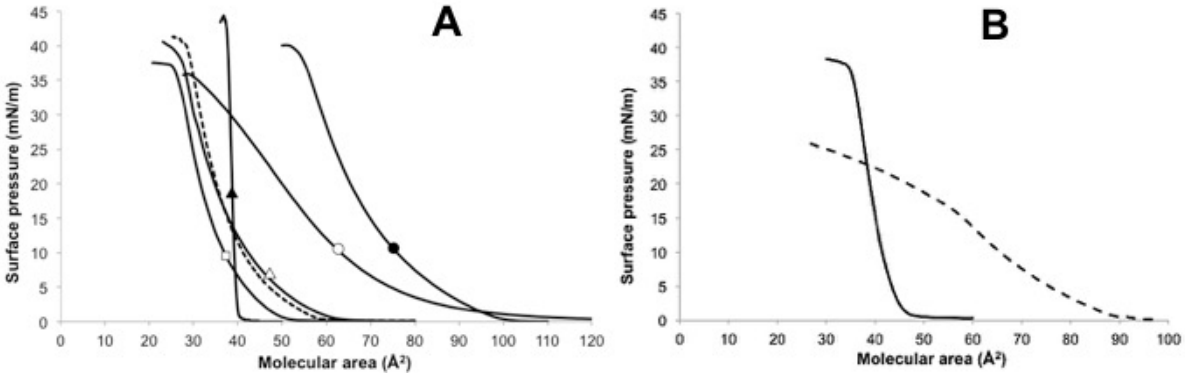

Figure 5

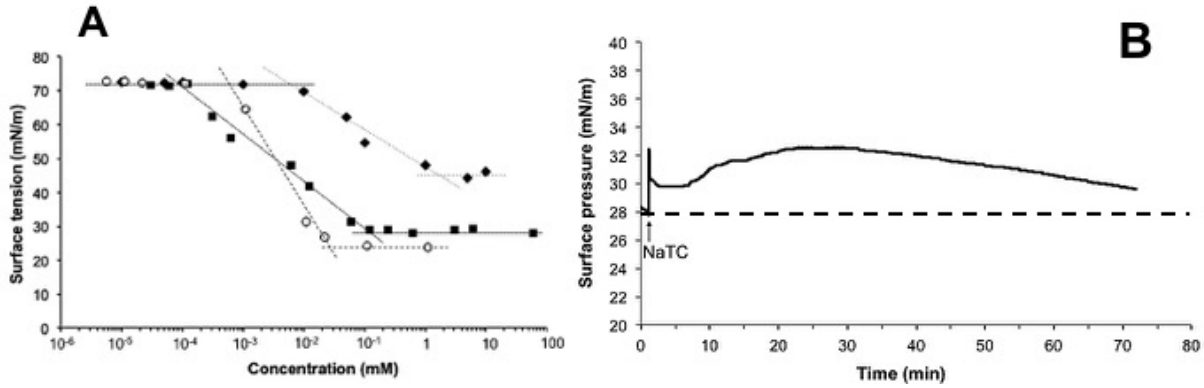

Figure 6

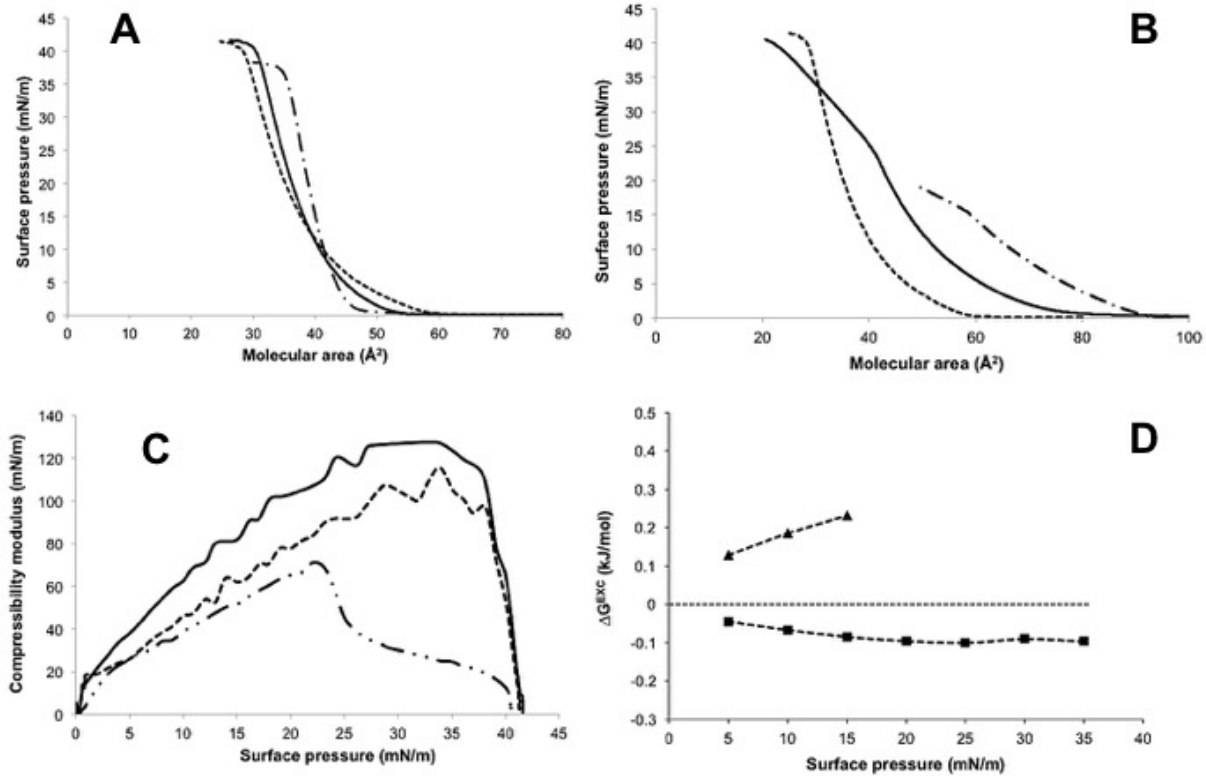

Highlights :

- Cholecalciferol D_3 exhibits dramatic solubilization in simulated intestinal medium
- Both lipids and bile salt in mixed micelles contribute to D_3 solubilization
- D_3 self-association is an additional factor impacting the solubilization process
- Retinyl palmitate (RP) is poorly solubilized in the mixed micelle solutions
- High excess free energy of mixing of RP with the lipids explains its poor inclusion